JOURNAL OF PROPULSION AND POWER
Vol. 14, No. 1, January–February 1998

Thermal Decomposition of 3,3′-Bis-Azidomethyl-Oxetane

Young Joo Lee,* Ching-Jen Tang,† Gautam Kudva,† and Thomas A. Litzinger‡
Pennsylvania State University, University Park, Pennsylvania 16802

Measurements of gaseous species and temperature profiles were performed to study the thermal decomposition of 3,3′-bis-azidomethyl-oxetane (BAMO). Experiments were conducted at 1 atm of argon with heat fluxes of 100 and 400 W/cm^2, delivered by a CO_2 laser. Gaseous samples were extracted through the use of a quartz microprobe and analyzed by a triple quadrupole mass spectrometer. Temperature profiles were measured using the microthermocouple technique to investigate gas-phase reaction zones identified by the species measurements. Flame structure and surface behavior were observed using a high-magnification video system. Major species evolved from the surface were identified as N_2, HCN, H_2CO, H_2O, NH_3, CO, and CH_4. Minor species include NO, H_2CNH (m/z = 29), CH_3CN(41), CH_3CHNH(43), C_2H_3CHO(56), $CO(CH)_2NH$(69), and C_2H_2. From the species measurements, at both experimental conditions, BAMO was found to undergo simultaneous decomposition of its backbone structure, indicated by the release of high concentrations of H_2CO, H_2O, and CO, and of side chains, by the large amounts of N_2, HCN, and some larger molecules. No gas-phase reaction was identified, because most of the major species measured exhibited relatively constant concentrations in the gas-phase. The lack of a gas-phase reaction was also evident from the gas-phase temperature profile that showed a constant value of approximately 1050 K.

Introduction

IN the search for new energetic binder materials, a great deal of interest has recently centered on azido compounds,[1] and one of those is 3,3′-bis-azidomethyl-oxetane (BAMO) (Fig. 1). BAMO draws considerable interest because it has potential as an energetic binder and a plasticizer in gun and rocket propellants, where a relatively low flame temperature and high mass impetus are desirable. Despite considerable interest, a limited number of research results have been published on the decomposition of BAMO.

A mass spectrometric kinetic study on the thermal decomposition of BAMO and other azide polymers was made by Farber et al.[2] The polymer samples, weighing 5–50 mg, were placed in a small capsule within an effusion cell, which was heated by a resistance furnace. Experiments were performed at temperatures from 60 to 300°C and at a pressure of 10^{-7} torr, and all mass spectra were obtained at an ionization voltage of 20 eV. During isothermal experiments,[2] the melting temperature of the BAMO polymer was found to be 75°C. Slight decomposition began at 130°C, and at that temperature the release of N_2 from azide groups was observed to be the primary decomposition path, where the rate of N_2 release increased as the temperature increased. The three-carbon backbone of the polymer remained intact until a higher temperature, approximately 160°C, when the mass spectrometer (MS) showed peaks of HCN, H_2, CH_2, CH_3, O, OH, H_2O, H_2CO, CH_2OH, and NO_2 in addition to N_2. These species showed the initiation of secondary decomposition.

BAMO monomer and polymer were investigated by Brill and his co-workers[3–5] with the rapid-scanning Fourier transform infrared (RSFTIR) spectroscopy technique to characterize the slow (5 K/min) and rapid (50–255 K/s) thermolysis of these compounds[3] and with the simultaneous mass and temperature change (SMATCH)/FTIR spectroscopy to determine the kinetics of weight-loss process of the compounds.[4] The RSFTIR spectroscopy was applied at pressures up to 69 atm and at high heating rates approaching those of rocket motor conditions, with a final temperature range of 640–950 K. For the slow thermal decomposition of the polymer,[3] N_2 was observed to be eliminated in advance of fragments originating from the polymer backbone by the observation of N_3 bands, consistent with the low pressure effusion cell-mass spectrometry experiment.[2] The destruction of the azide group was accompanied by the growth of intense bands from species such as amide, amine, imine, and oxime, although the polymer backbone remained essentially unchanged after the azide bands completely disappeared. For the high heating rate thermolysis, however, the rupture of the backbone was apparently identified by the products of HCN, CO, H_2CO, NH_3, and several hydrocarbons.

From a study of the kinetics and near-surface products of BAMO,[4] the heat release during decomposition of azide polymers was found to increase with the weight fraction of the azide group in the polymer, which indicated that the azide group controls the overall decomposition energy release kinetics through the following reaction:

$$RN_3 \rightarrow RN + N_2 \qquad (1)$$

The nitrene intermediate, RN, is unstable and reacts further to produce more stable species, e.g., HCN and NH_3, which are major products. Because the nitrene functional group in reaction (1) is formed in the methylene azide side chain of BAMO, the formation of HCN and NH_3 indicates that the nitrene has two decomposition branches: dominant C–C fission caused by the high concentration of HCN, and lesser C–N fission for liberating NH_3. These two decomposition branches were also observed from the products coming from the residual nitrene, RCH_2N, in experiments at temperatures between 275 and 390°C.[5] In the experiments, BAMO produced CO and H_2CO along with HCN and NH_3, and all of these products formed from reactions associated with the condensed phase at high heating rates. However, the branching trend and overall reactions were found to be independent of temperature in the range studied.[5]

BAMO polymer and copolymer with tetrahydrofuran (THF) were studied by Miyazaki and Kubota[6] to examine their phys-

Received March 4, 1997; revision received Aug. 5, 1997; accepted for publication Aug. 6, 1997.

*Post-Doctoral Research Associate.
†Graduate Research Assistant.
‡Professor, Department of Mechanical Engineering, Pennsylvania State University, University Park, PA 16802.

icochemical properties using differential thermal analysis (DTA) and thermogravimetric analysis (TGA).[6] The BAMO polymer sample was a pressed pellet, 7 mm in diameter and 10 mm in length, and ignition of the sample was achieved using an electrically heated nichrome wire. The TGA data revealed that the first-stage weight loss occurred rapidly at about 187°C and was completed at about 247°C with the approximately 35% weight loss. This stage was predominantly related to the elimination of the N_3 bond in the infrared (IR) spectra of the sample. The second-stage weight loss process occurred slowly without heat liberation and was caused by the decomposition of remaining fragments as detected by the strong IR absorption of C═N, C—H, and C—O bonds. Considering that the total mass fraction of N is 50% in BAMO polymer and that N_2 is an inactive species for IR, a significant amount of N was believed to be evolved as N_2 molecules at the second stage. From the studies of the combustion characteristics of BAMO in the pressure range of 10–40 atm,[6] it was observed that the gasification reaction was terminated when the external heating was removed.

Although the initial decomposition pathways in the condensed phase of BAMO were suggested from the previous experimental studies,[2–6] no further gas-phase decomposition processes after the initial stage were identified. Moreover, there exists some discrepancy of the gaseous species evolved in the initial decomposition pathways from the previous studies: N_2, HCN, H_2, CH_2, CH_3, O, OH, H_2O, H_2CO, CH_2OH, and NO_2 in the low-pressure mass spectrometric study,[2] and N_2, HCN, CO, H_2CO, NH_3, and several hydrocarbons in Fourier transform infrared (FTIR) experiments.[3–5] Considering that the initial decomposition species determine subsequent gas-phase reactions and species production, accurately identifying major gaseous products evolved from BAMO decomposition is extremely important. Therefore, in this study, the thermal decomposition of BAMO was investigated at high heating rate conditions that can approach rocket motor conditions; major emphases were placed on the identification of decomposition products at the surface and in the gas-phase, and the accurate quantification of the measured species. Using these results, along with the information from temperature profiles, the chemical and physical structures of gas-phase BAMO decomposition were examined.

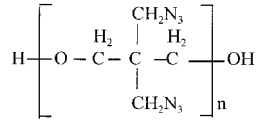

Fig. 1 Chemical structure for the BAMO polymer.

Experimental Approach

Experimental Setup

The experimental apparatus is basically composed of a high-power CO_2 laser used as the radiant heat source of BAMO propellants, visual diagnostics for the examination of flame behavior and species sampling height, a TQMS and related electronics for gaseous product analysis, and a data acquisition and analysis system. The schematic diagram of the experimental setup is shown in Fig. 2, and a detailed description will be given here.

The energy source for ignition and sustained combustion of BAMO propellant samples was a Coherent Super 48 high-power CO_2 laser with a maximum of 700 W of continuous wave power. A series of silicon mirrors directed the beam from the laser to the test chamber through aluminum tubes that safely confine the high-power CO_2 laser beam. Before entering the test chamber, the beam passed through a drilled copper plate and then through an expanding lens, both of which are mounted on sliding mounts movable on a vertical aluminum track directly above the test chamber. A 7-mm aperture in the center of the copper plate allows only the more uniform center section of the beam to be passed onto the sample surface. A zinc selenide expanding lens with a focal length of 24 cm can be moved on a track (not shown in Fig. 2) to expand the beam to the desired area and thus obtain various levels of incident heat flux. The laser beam enters the test chamber through a KCl window and is applied on the propellant sample surface. The test chamber shown in Fig. 2 was made from 1.3-cm-thick aluminum, and was 25.4 cm tall and 16.5 cm on a side to give an internal volume of 4460 cm^3. Four pipe-thread fittings were installed in the chamber to allow control of the pressure and gaseous environment in the test chamber and data transmission. Two fittings allow for gas flow from pressurized bottles containing the environmental gas (Ar or N_2) and provide gas flowout induced by a vacuum pump. The other two feedthroughs were connected in two other fittings (not shown in Fig. 2) to transport the photodiode and thermocouple signals out of the chamber. These fittings were specially designed for sealing signal-transmitting wires and were purchased from CONAX Buffalo Co.

The propellant samples were 0.64-cm (0.25-in.) diameter pellets pressed from BAMO powder by the in-house, pellet presser. For a test, the propellant sample was glued to a small

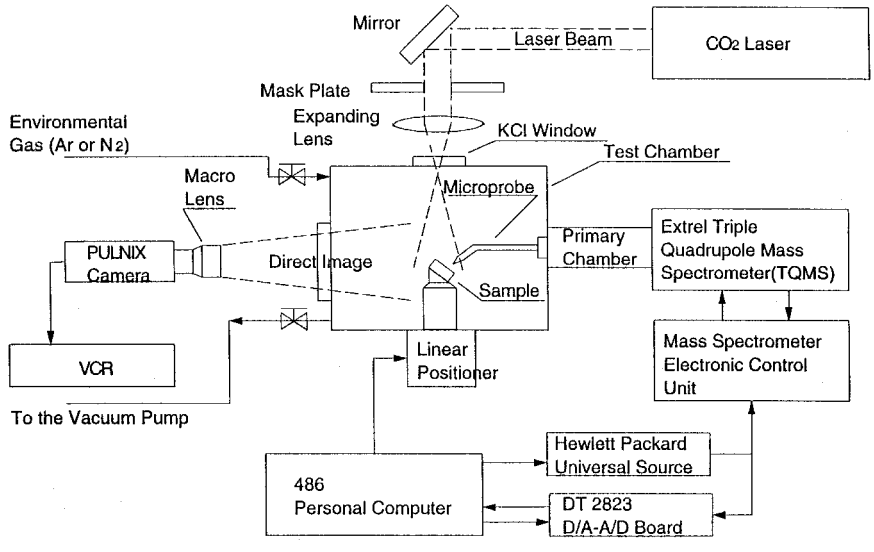

Fig. 2 Schematic diagram of the experimental setup for the decomposition study of BAMO propellants in the gas-phase using microprobe/triple quadrupole mass spectrometer.

sample holder, angled at 45 deg to the incident laser beam so that the sampling microprobe could approach the sample perpendicular to the center of the sample surface. This sample holder was attached on a linear positioner from Industrial Devices Corp., which permitted precise vertical positioning and movement of the test sample with respect to the position of the sampling probe orifice. During a test, the sample is pushed toward the sampling probe by the linear positioner to obtain species profiles vs height from the sample surface. A high-quality Plexiglas® window was installed on one side of the chamber for direct image photography of the BAMO flame during combustion. The direct image was acquired using a Pulnix video camera with a Nikon macrolens and recorded with a professional VCR model BV-1000 from Mitsubishi, Inc. Magnification of 30 to 40 times was normally employed to record images of flame structure and to obtain the sampling height with the spatial resolution of about 20 μm. The recorded images were examined frame-by-frame to identify the sampling height with the help of separately recorded photodiode signals. The signals were recorded from a photodiode installed at a corner in the test chamber for simultaneously identifying the onset of the sample flame and the burning behavior of the propellants.

Sampling of gaseous species was performed using a microprobe/mass spectrometer (MPMS) system. The species were sampled by a quartz microprobe with an orifice diameter of 20–30 μm and a nozzle half-angle of 15–20 deg. The microprobe was constructed with quartz tubing of 2.0 (i.d.) × 3.2 (o.d.) mm from Quartz Scientific, Inc., which was placed in a lathe and spun at low rpm while being heated by a small torch and pulled to create a narrower neck. The tubing was then cut at the narrowest point, and the point of the tip was then carefully ground back until an orifice of the desired size was obtained. The sample gases were drawn into the MS by a set of turbomolecular pumps and vacuum pumps and ionized by electron impact in the MS. The mass spectrometer unit is a C-50 TQMS from Extrel, which is capable of analyzing gaseous species in the mass range of 1–500 amu with optional high-mass analysis power and has a variable scan speed between 0.2 and 1000 amu/s. A resolution of 8000 is obtainable at a mass of 500 amu and 4000 at 28 amu, and the sensitivity is 4 MA/torr at mass 28 amu before electronic amplification. A two-stage pumping system was employed to obtain the required low pressures for the MPMS system. The vacuum conditions for the primary and secondary probe chamber of the TQMS system were achieved with a backing pump from Leybold and two turbomolecular pump units from Balzers. The secondary probe chamber containing the TQMS unit is pumped down to a pressure of about 10^{-6} torr for normal sampling conditions. A Pirani gauge and a cold cathode gauge are employed to measure the pressures in the primary and probe chambers, respectively. The vacuum housings and flanges that house the TQMS and seal the MPMS system were purchased from MDC Vacuum Products Co. The ionized gas samples were directed to the detection system of the TQMS where they are detected and the signals are amplified. The data were collected and analyzed using a 486-based personal computer and custom analysis software.

Species Measurement and Analysis

Identification of species and differentiation of several possible species with the same mass-to-charge ratio (m/z) value were performed using the TQMS. Two modes can be selected for the mass filtering operation of a C-50 TQMS: a parent mode and a daughter mode. In parent mode operation, which is the same as with a single quadrupole mass spectrometer (QMS), the existence of a gaseous species was identified by peaks at various mass values that were detected only using the first ($Q1$) or third ($Q3$) quadrupole mass filters of the TQMS. However, if multiple species exist at a given mass, differentiating these species is very difficult only using the parent mode; it requires multiple runs at different ionization energies or the application of a matrix approach for obtaining quantitative data. Therefore, the daughter mode operation with the use of all functions of the TQMS is especially powerful in differentiating and identifying several species with the same mass.

In daughter mode operation, the first quadrupole mass filter ($Q1$) is operated in a single ion mode in which only the ions of interest are allowed to pass on as parent ions. The selected parent ions undergo dissociation through the process of collision induced dissociation (CID) in the second mass filter ($Q2$). Argon was used as the collision gas in this study to minimize its contribution to fragmented masses. Several possible fragmented mass ions, called daughter ions, are produced and delivered into the third mass filter ($Q3$). Here, all possible daughter ions for each parent ion were scanned and directed into the detection system as in the parent mode. Two different types of daughter mode experiments were performed with different levels of collision energy; they will be referred to as the high- and low-energy modes.[7] In the high-energy mode, the collision energy is sufficient to break double bonds or even triple bonds of the parent ion. In the low energy mode, the energy is only enough to break the weakest bonds of the parent ion so that daughter ions deprived of small numbers of outer atoms are produced. The low energy mode operation was especially useful when more than three species were possible and/or several hydrocarbon compounds could exist at the same mass. Based on the two sets of daughter mass ions for each parent mass, the most appropriate chemical formula of the parent mass was then deduced from the comparison of daughter ion patterns between the measured parent mass and a presumed chemical species, literature published on the propellants, and a library of mass spectra.[8] Based upon procedures for identification and differentiation of species established previously,[9–11] the differentiation of species with the same mass was performed for mass 28: N_2, CO and C_2H_4; mass 29: H_2CO and H_2CNH; and mass 30: NO, H_2CO, and C_2H_6. No differentiation for mass 44 (possibly, N_2O, CO_2, or CH_3CHO) was attempted because the signal intensity of mass 44 was negligible for both experimental conditions.

Sensitivity coefficients of the measured species were acquired by several calibration methods. The most stable species were calibrated directly with the gas mixtures of known concentration. Water (H_2O), acetonitrile (CH_3CN), acrolein (C_2H_3CHO), and pyruvonitrile (CH_3COCN), which are liquid at standard conditions, were heated and vaporized with the CO_2 laser to obtain sensitivity coefficients for their vapor states. Paraformaldehyde, a polymeric solid of formaldehyde (H_2CO), was used to calibrate H_2CO. The calibrations of species for which standards were not readily available were estimated by correlating the signal intensity to that of calibrated species with a similar appearance potential through the ratio of their cross sections.[12] For all of the calibrations and actual tests, an ionization energy of 22 eV was used to minimize the fragmentation of molecules and to get acceptable intensities. However, this setting was still high compared to the ionization energies of 9–15 eV for most organic compounds; thus, some fragments were formed and contributed to the signals at masses other than the parent mass. In such instances, these fragment signals were subtracted from the mass signal of interest.

In the present study, experiments for BAMO were conducted at the pressure of 1 atm and at heat fluxes of 100 and 400 W/cm^2 during laser-assisted combustion. In reducing the species data, the measured concentrations were summed and each concentration was divided by the total to get the mole fractions of the sampled gases. This method of calculating normalized mole fractions eliminates the effect of sample temperature on the observed signal intensities, because the temperature dependence cancels out. This calculation method also cancels out the effect on signal intensity of probe orifice blockage during

a test. The measured mole fractions were then used to perform element balances through the reaction zones as a check on the quality of the data.

Temperature Measurements

Temperature profiles for BAMO pellets were recorded for analyzing the combustion wave structure during deflagration and, hopefully, the relationship between chemical reactions and the thermal wave structure through comparison of the species and temperature measurements. Temperatures at the surface and in flame zones were measured using 25 μm diameter platinum–rhodium (Pt/Rh) and tungsten–rhenium (W/Re) thermocouples. A Nicolet NIC-310 digital oscilloscope was used to record thermocouple signals. The scope operates at a maximum recording speed of 1 MHz and has two input channels; one channel was for thermocouple signals and the other one for IR photodiode signals. The photodiode signals were simultaneously recorded with the temperature signals to synchronize the video images containing flame behavior to the temperature measurement.

Results and Discussion

Identification and Differentiation of Measured Species

Major parent mass signals and related daughter masses for the decomposition products of BAMO propellants are presented in Table 1. The most probable structure of each parent mass was determined and included in Table 1, based upon the two sets of daughter masses from daughter mode experiments. Three species were found in mass 28: N_2, C_2H_4, and CO; however, N_2 was identified to be the dominant species at the present experimental conditions as shown in Fig. 3. Mass 27 was composed of HCN and a small amount of C_2H_3. Most daughter masses in high- and low-energy modes from C_2H_3 may overlap those from HCN. However, the amount of C_2H_3 can be estimated from the parent mass calibration of C_2H_4, since C_2H_3 is a large fragment from C_2H_4 in the parent mode. Therefore, the amount of HCN can be calculated by deducting the amount of C_2H_3 from the total intensity of mass 27. The C_2H_3 is most likely a fragment formed during ionization from C_2H_4 because the present sampling system is not designed to measure radicals. Both H_2CO

Table 1 Daughter mass ions for each major parent mass of BAMO propellants at 1 ATM and 400 W/cm^2 [a]

Parent mass	High-energy mode	Low-energy mode	Most probable chemical structure
28	14, 12, 15	27 >> 26[b]	N_2, C_2H_4, CO
27	N/A[c]	26 > > 25, 24	HCN >> C_2H_3
30	14 only	29 >> 28	H_2CO
29	13, 14, 12	28	H_2CNH, CHO
39	13, 18, 14, 16, 28 (all small amount)	38, 37	No matching stable species was found
41	15, 14, 27 >> 26, 28, 13	40 >> 39	Fragment from mass 43, CH_3CN[d]
42	27, 15, 26, 14, 28, 26	41, 40 >> 39	Fragment from mass 43
43	27, 15, 28, 29, 26 >> 17, 14	42 >> 41, 40	CH_3CHNH
18	N/A	N/A	H_2O
17	N/A	16 >> 15	OH >> NH_3
54	27, 28 >> 39, 26, 29	53 (small amount)	$CH_2(CH)_2N$• radical
55	28, 29, 27, 39, 26	51, 50 >> 49	Fragment from mass 56
56	28, 29, 30, 39, 27, 41, 15	55, 54, 53 (all small)	C_2H_3CHO
69	(1) 28, 30, 29, 39[e] (2) 30, 28, 29, 27, 39	68	$CO(CH)_2NH$ or CH_3COCN[f]

[a] Mass ions are placed in the order of descending intensity.
[b] The signal at mass 27 is larger than that at mass 26 by at least one order of magnitude.
[c] Data was not obtained since the expected information was not prerequisite for this study.
[d] Mass 41 is composed of fragments from mass 43 (CH_3CHNH) and CH_3CN.
[e] Two possible combinations of daughter masses were obtained from experiment; however, combination (1) is more frequent.
[f] $CO(CH)_2NH$ is better than CH_3COCN in matching combination (1).

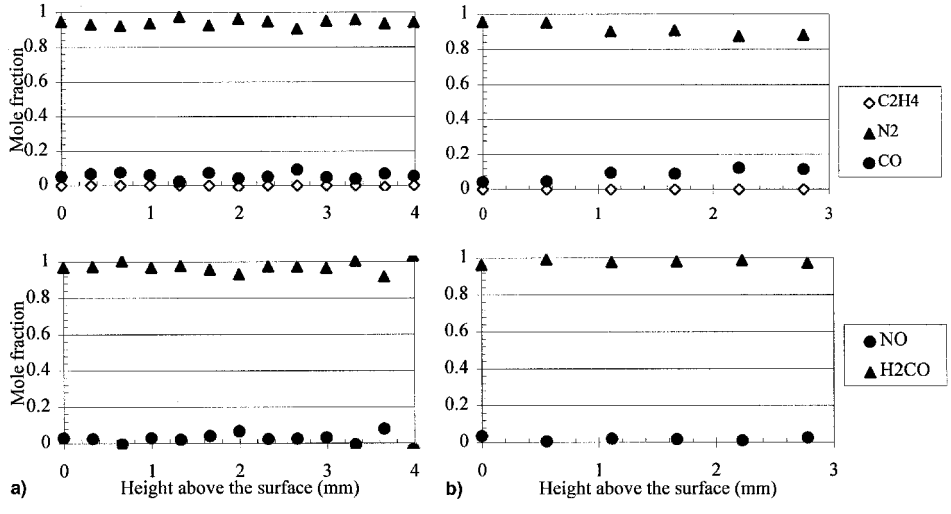

Fig. 3 Relative concentration of species for mass 28 and 30 in the gas-phase of BAMO propellants at the heat flux of a) 100 and b) 400 W/cm^2 at 1 atm in argon environment.

and NO exist at mass 30; however, H_2CO was dominant, as shown in Fig. 3. In the present study, mass 29 was found to be composed of CHO and H_2CNH; both species seem to contribute equally to the signal intensities of mass 29 based upon available calibration results.[9] At mass 29, CHO is a fragment from H_2CO. However, H_2CNH may be a stable intermediate decomposition product or a stable ionization fragment from a larger molecular species as in RDX.[9,13] Although the presence of H_2CNH was not confirmed as a decomposition product by other experimental studies,[2–5] based on the BAMO structure (Fig. 1), H_2CNH is believed to be an actual decomposition species produced from the side-chain following N_2 elimination. Mass 18 is believed to totally consist of H_2O; therefore, no special analysis was undertaken for the mass. Mass 17 is composed of NH_3 and OH, which comes from the fragmentation of H_2O in the ionizer; therefore, the quantity of NH_3 was calculated by deducting the portion of the OH fragment from the total intensity of the mass 17.

Most of the major species measured in this study were also found in other measurements, except H_2CNH.[2–5] In the low-temperature (80–250°C) effusion cell-mass spectrometer experiment,[2] major products were measured at mass 28, 27, 30, 29, and 18, and they were attributed to N_2, HCN, H_2CO, CHO (fragment from H_2CO), and H_2O, respectively. However, no measurement of CO and C_2H_4 in mass 28 was reported in the reference. Many of the same major species such as HCN, H_2CO, NH_3, and CO were found in FTIR experiments at various heating rates,[3–5] except for N_2 and H_2O, which were not measured and quantified. It is noteworthy that CO and C_2H_4 were measured as major species for mass 28 from the FTIR experiments, while, in this study, mass 28 was predominantly composed of N_2, with very little CO and C_2H_4 (Fig. 3). However, the relative concentrations of three species for mass 28 from the FTIR experiments could be similar to those from this study because a high mole fraction of N_2 is expected based upon quantities of other species from the FTIR measurements and the structure of BAMO (see Fig. 1). C_2H_2 and CH_4 were reported as major species from reactions in the condensed phase of the BAMO decomposition from the FTIR experiments with high heating rates[3–5]; however, both species turned out to be minor in the present study. All of these differences in measured major species seem to be primarily a result of the difference of experimental conditions, especially of heating rates. Because the effusion cell-MS study[2] was conducted at the heating rate of 1 K/s and very low pressures, major species included H_2 and unstable radicals such as CH_3, CH_2, and OH, which require few bond fractures and little H atom migration. In the FTIR studies with moderate and high heating rates up to 255 K/s,[3–5] NH_3 and many stable hydrocarbons such as CH_4, C_2H_2, and C_2H_4, which require more migration and recombination reactions by H atoms, were measured. In the present study, where the heating rates are at least one order higher than those in the FTIR studies, even more H migration and reaction is present; as evidenced by higher concentration of NH_3 and H_2CO, without any significant change of other major species [see Eqs. (3) and (4) for comparison].

Besides the previously mentioned species, which were measured in both present work and previous studies,[2–5] other masses that were not measured or were minor in previous studies were also found in the present study. CH_3CHNH seems to be the only possible stable species at mass 43, and its chemical structure is suggested in Fig. 4.[9,13] No possible arrangements with a molecular formula C_2H_5N including CH_3CHNH were commercially available[14]; therefore, no direct calibration evidence for the daughter mass distribution of CH_3CHNH could be obtained for comparing with the measured daughter masses of the mass 43 in Table 1. However, by analysis of the distribution of daughter mass ions from the species with similar chemical structures,[9,10] a likely stable chemical structure could be suggested. It may be noteworthy that mass 43 was also measured in the low-temperature effusion cell-MS study[2] as a product from AMMO (3-azidomethyl-3-methyloxetane), another oxetane binder, by backbone scission, and C_2H_3O was assigned to this mass. However, C_2H_3O seems to be a radical with the following chemical structure and is not probable for the mass 43 measured in BAMO decomposition.

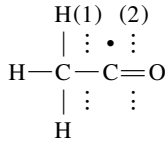

The most abundant daughter masses from this radical are probably mass 15 or 28 by the C—C bond breaking, (1) in the preceding chemical structure, based upon the daughter mass distribution from CH_3CHO.[9] The evolution of daughter mass 27, which is the most abundant for the mass 43 (see Table 1), by the scission of C=O bond, (2), turned out to be much less probable from the same data.[9] On the other hand, according to the daughter mass pattern from CH_3CN, which has a similar structure to CH_3CHNH,[9] the production of daughter mass 27 from CH_3CHNH is relatively easy by the breaking of C=N or C—C bonds and the H migration from either side of the disconnected parts (see Fig. 4). Therefore, it may be concluded that C_2H_3O is not a possible species for mass 43 in the present study. By the same analysis, mass 42 was determined to be an ionization fragment from CH_3CHNH by breaking one of the weakest bonds, H—C. Although much similarity exists among daughter masses from mass 41 to 43 in Table 1, mass 41 seems to consist of two species: a stable fragment from mass 43 (I) and CH_3CN (II), acetonitrile, as in Fig. 4.[9,13] At this stage, however, the relative amount of each species cannot be estimated.

Mass 56 is another species that was measured in this study, but in no other experiments.[2–5] The most probable species for this mass is C_2H_3CHO, acrolein, based upon the comparison of current daughter masses (Table 1) with those from C_2H_3CHO.[9,13] Other plausible candidates only composed of C,

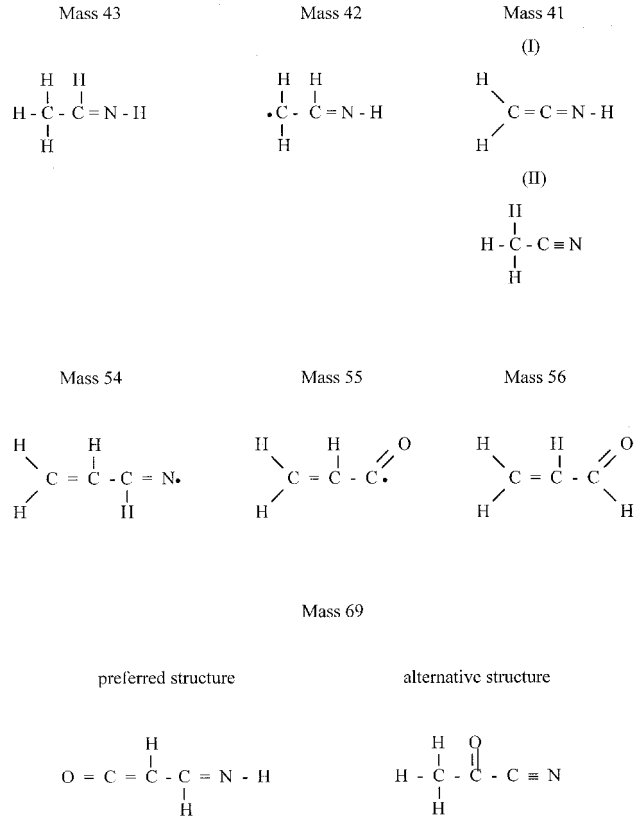

Fig. 4 Suggested chemical formula for masses at 41, 42, 43, 54, 55, 56, and 69.

H, O, and N atoms, were also examined for mass 56, based upon their chemical structures and possible daughter masses that could be produced according to available references.[8,14] However, no other species appeared to be a plausible candidate. The chemical structure of C_2H_3CHO is also shown in Fig. 4. Mass 55 seems to be a direct fragment from C_2H_3CHO, mass 56, with the structure shown in Fig. 4, because the daughters from mass 55 can be easily traced by those from acrolein, C_2H_3CHO (Table 1). Mass 54 was originally thought to be a fragment, C_3H_2O, from a radical, $C_2H_3CO\bullet$, because of the similarity of these daughter masses; however, the daughter mass 27, HCN or C_2H_3, could not possibly be obtained from any arrangements of the mass 54. No stable structure can be made for mass 54 with only C, H, O, and N atoms; the only possible species seems to be $CH_2(CH)_2N\bullet$, a radical, for satisfying the daughter masses presented in Table 1 and the existence of a major source of the measured daughter mass 27. $CH_2(CH)_2N\bullet$ seems to come from breaking the backbone and retaining one N atom of the azido groups in BAMO (Fig. 1). Mass 69 presents another decomposition species that was measured only in this study, without any measurement reported in other studies. Two different sets of daughter masses were measured in the present experiments[9,13]; however, the first set, (1) in Table 1, is considered more reliable than (2) because it contained less noise. $CO(CH)_2NH$ seems to be a better structure for mass 69 than CH_3COCN, pyruvonitrile, because obtaining mass 28 as a most abundant daughter is more direct from $CO(CH)_2NH$ in the high-energy mode, based on their chemical structures (Fig. 4). Moreover, the ordering of the heavy atoms in the proposed structure is consistent with their ordering in BAMO.

In this study of BAMO decomposition, no signal was measured at mass 46, and mass 44 was too small in intensity to be considered even as a minor product. Several mass signals in the mass 40 to 48 range were recorded in the effusion cell-MS study,[2] but all of the products were estimated to be formed as a result of effusion cell reactions, not because of the BAMO decomposition. Therefore, no assignment of species or their chemical structures was given to the masses between 40 and 48 amu in this study.

Species and Temperature Profiles in the Gas-Phase

The results of species measurements for BAMO pellets at 100 and 400 W/cm^2 and 1 ATM are shown in Figs. 5 and 6, respectively. Note that, in these figures, a different scale was used on the right side of the vertical axis to accommodate species with higher concentrations. Major species for the BAMO decomposition in the gas-phase are N_2, HCN, H_2CO, NH_3, H_2O, CO, and CH_4 in descending order. Minor species include NO, H_2CNH (m/z = 29), CH_3CN(41), CH_3CHNH(43), C_2H_3CHO(56), $CO(CH)_2NH$(69), and C_2H_2. The quantities of CH_3CHNH and $CO(CH)_2NH$ were estimated using sensitivity coefficients calculated from the cross section method.[12] The same masses and similar order of intensities were measured at the two heat flux conditions, except for NH_3, the mole fraction of which increased from 0.05 at 100 W/cm^2 to 0.11 at 400 W/cm^2. Therefore, the same basic interpretation can be applied for the chemical and physical processes of BAMO decomposition at both experimental conditions.

Species measured at the surface from the two test conditions (Figs. 5 and 6) can be classified into two categories: species produced from bond-breaking in the side-chains, e.g., N_2, HCN, NH_3, and H_2CNH, and from the rupture of the three-carbon backbone, e.g., H_2CO, H_2O, and CO (Fig. 1). Therefore, these results clearly show that the BAMO decomposition at the surface occurs simultaneously from bond-breakings in the side-chains and the backbone. Moreover, all BAMO decomposition products maintain their concentrations away from the surface, indicating a lack of further gas-phase reactions.

The decomposition of BAMO seems to be dominated by condensed phase chemistry, because the surface mole fractions of most species are similar to those in the gas-phase and no further gas-phase reaction was observed. All possible decomposition

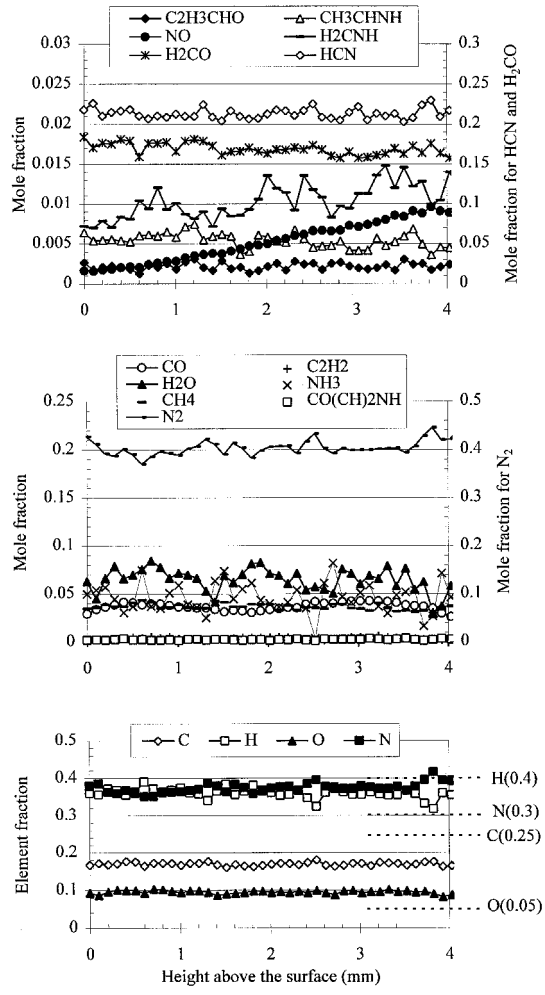

Fig. 5 Species profiles for BAMO at 1 atm and 100 W/cm^2 in argon environment.

reactions seem to be completed in the condensed phase, and most of the energy related to the decomposition is already released from the rupture of azide group in producing N_2.[4,5] This energy is the major source of the temperature rise to a final gas-phase temperature, 1000–1100 K, for BAMO (Fig. 7). Although species such as H_2CO and HCN, which are reactive at this temperature, exist in the gas-phase (Figs. 4 and 5), no oxidizing species such as NO_2, N_2O, or NO[9,10] exist to allow further reaction. Thus, H_2CO and HCN can maintain high gas-phase concentrations without experiencing any consumption reactions.

For species measurements in Figs. 5 and 6, the element atom balances for carbon were low. Considering that the sum of the signal intensity of each species quantified in Figs. 5 and 6 represents somewhat less than 80% of the total intensity of all signals in the measurements, it is possible that solid carbon[6] and/or some of hydrocarbon-containing radicals or species in small quantities might not have been measured in this study.

With the species profiles in Fig. 5 at 1 atm and 100 W/cm^2, the overall decomposition pathway for BAMO at the surface can be postulated as follows:

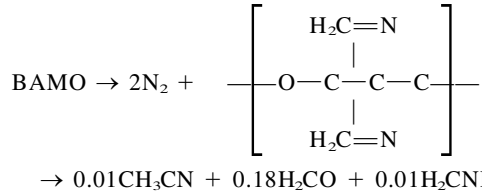

$$\rightarrow 0.01CH_3CN + 0.18H_2CO + 0.01H_2CNH + 0.41N_2 + 0.03CO + 0.22HCN + 0.06H_2O + 0.05NH_3 + 0.04CH_4 \quad (2)$$

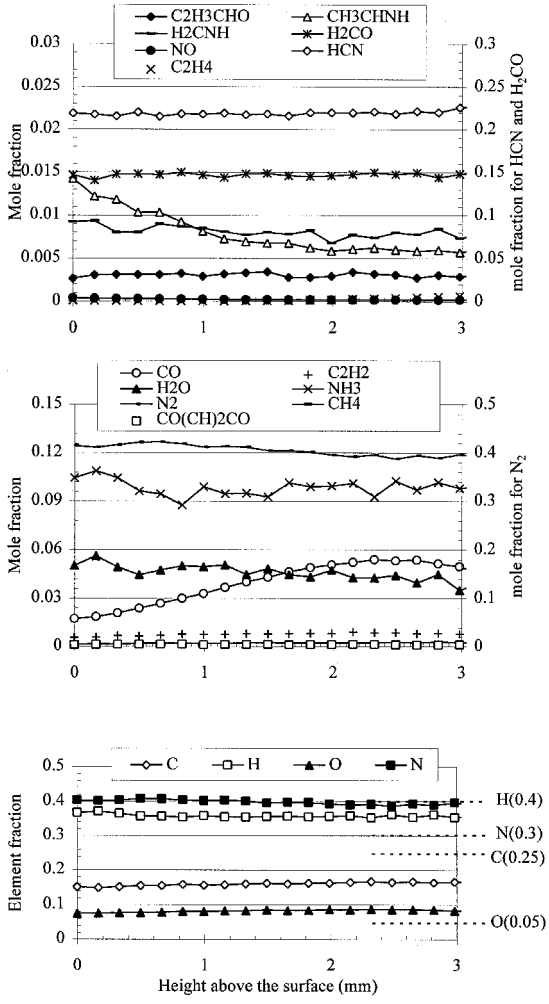

Fig. 6 Species profiles for BAMO at 1 atm and 400 W/cm^2 in argon environment.

In this pathway, C_2H_4, C_2H_2, and high molecular weight species shown in Fig. 5 were not included because of very small mole fractions of the species. To confirm the reliability of the present data, the species result at 1 atm and 100 W/cm^2 was compared with the data at the highest heating rate (255 K/s) in FTIR study.[4] Only considering the species measured in the FTIR study and renormalizing those, the decomposition pathway for BAMO at the surface can be compared between this study [Eq. (3)] and the FTIR study [Eq. (4)]:

$$\text{BAMO} \rightarrow 0.35H_2CO + 0.01C_2H_2 + 0.06CO + 0.42HCN + 0.10NH_3 + 0.08CH_4 \quad (3)$$

$$\rightarrow 0.08H_2CO + 0.06C_2H_2 + 0.23CO + 0.42HCN + 0.08NH_3 + 0.08CH_4 + 0.05C_2H_4 \quad (4)$$

Similar major species were identified in both studies; however, in this study, a much higher concentration was obtained for H_2CO and a lower concentration for CO, both of which are major species produced from the backbone of BAMO. C_2H_4 and C_2H_2, which were measured as major products in the FTIR experiments,[3–5] are small in this study. Therefore, these results suggest that, because of much higher heating rates in this study, the production of the species such as H_2CO and NH_3, which are formed from species more bond-breaking and/or H atom migration, are preferred over CO, C_2H_4, and C_2H_2 in the FTIR studies.[3–5]

It was possible that the higher concentration of NH_3 measured at 400 W/cm^2, compared to the data at 100 W/cm^2 in this study and from FTIR experiments,[3–5] was related to a possible effect of water in the BAMO propellant samples before tests.[15] Therefore, some tests were conducted for both conditions with the samples that were dehydrated for several days to exclude any possible water contamination to the propellants. No substantial change of order and quantities of the measured major species were observed for either condition, but some decrease of the surface mole fraction of NH_3 was observed from ~0.14 to ~0.11 at 400 W/cm^2. Therefore, the influence of water seems to be minor on species profiles, and the higher quantity of NH_3 at 400 W/cm^2 appears to be accurate. The chemical reactions leading to the increased NH_3 are not known at this time.

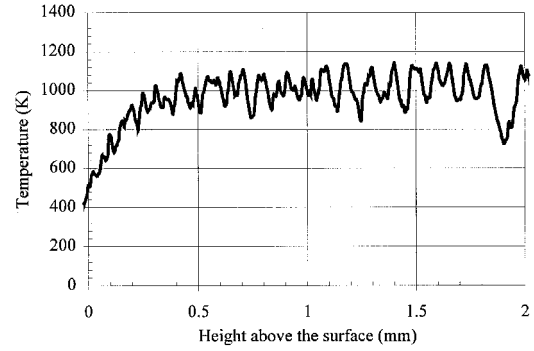

Fig. 7 Temperature profile for BAMO at 1 atm and 100 W/cm^2 obtained with a 25 μm W/Re thermocouple.

Weak blue flames were usually observed in the gas-phase throughout the experiments for both conditions. Burning rates of BAMO pellets were extremely high: 10.7 ± 2.0 mm/s at 400 W/cm^2 and ~3.4 mm/s at 100 W/cm^2. Moreover, regressing surfaces of the BAMO pellets were very sensitive to the distribution of the applied laser beam, so that the surfaces became uneven during combustion as a result of the slight nonuniformity in the distribution of the beam. This behavior related to high burning rates was the main source of poor temperature measurements in these experiments, especially at 400 W/cm^2. A typical gas-phase temperature profile is shown in Fig. 7 at the condition of 1 ATM and 100 W/cm^2. The surface temperature was 500–510 K and the profile reached a constant final temperature, 1000–1100 K, at ~300 μm above the surface. The species profiles at the same condition (Fig. 5) do not show any explicit changes related to the temperature rise near the surface. However, most of the unsuccessful temperature measurements starting from within the condensed phase showed very steep rises near the surface, and the intensities of all mass signals in this study showed transient values during the initial stage of the measurements. Therefore, it can be deduced that the rising portion of the temperature profile in Fig. 7 represents a transient response as a result of the onset of laser-ignition, since the temperature measurement started at the surface of the BAMO propellant sample. It is interesting that a similar temperature profile was reported in the combustion wave measurement of cross-linked BAMO/THF(6/4) copolymer at 20 ATM, in which THF (tetrahydrofuran) was used as a copolymer for easy curing process.[6]

Summary and Conclusions

A study of the thermal decomposition of BAMO polymers was performed through the measurements of gaseous species and temperature profiles. Major species evolved from the surface were identified as N_2, HCN, H_2CO, NH_3, H_2O, CO, and CH_4. Minor species include NO, H_2CNH (m/z = 29), CH_3CN (41), CH_3CHNH (43), C_2H_3CHO (56), $CO(CH)_2NH$ (69), and C_2H_2, most of which were not reported previously. Compared to other studies of BAMO,[2–5] the measurement of higher NH_3 and H_2CO in connection with a lower concentration of hydrocarbons and CO are probably because of the higher heating

rates that caused more bond fractures and H atom migration. From species measurements, BAMO was found to undergo simultaneous decomposition of its backbone structure, indicated by the release of high concentrations of H_2CO and CO, and the breaking of side chains, from the large amounts of N_2, HCN, and some larger molecules. The decomposition of BAMO seems to be dominated by condensed phase chemistry, because surface mole fractions of most species are similar to those in the gas-phase and no further gas-phase reaction was observed. This was also identified from the temperature profile in the gas-phase that was constant at approximately 1050 K.

Acknowledgments

This work was performed under the sponsorship of the Office of Naval Research, Mechanics Division, N00014-93-1-0080. The support and encouragement of R. S. Miller are greatly appreciated. Gerry Manser of Aerojet Tech Systems generously contributed BAMO powders for this study.

References

[1]Miller, R. S., "Research on New Energetic Materials," *Decomposition, Combustion, and Detonation Chemistry of Energetic Materials*, T. B., Brill, T. P., Russell, W. C., Tao, and R. B. Wardle, (eds.), Vol. 418, Material Research Society, Pittsburgh, PA, 1996, pp. 3–14.

[2]Farber M., and Srivastava, R. D., "Mass Spectrometric Kinetic Studies on Several Azido Polymers," *Combustion and Flames*, Vol. 55, 1984, pp. 203–211.

[3]Y. Oyumi and T. B. Brill, "Thermal Decomposition of Energetic Materials 12. Infrared Spectral and Rapid Thermolysis Studies of Azide-Containing Monomers and Polymers," *Combustion and Flame*, Vol. 65, No. 2, 1986, pp. 127–135.

[4]Chen, J. K., and Brill, T. B., "Thermal Decomposition of Energetic Materials 54. Kinetics and Near-Surface Products of Azide Polymers AMMO, BAMO, and GAP in Simulated Combustion," *Combustion and Flame*, Vol. 87, 1991, pp. 157–168.

[5]Brill, T. B., and Brush, P. J., "Condensed Phase Chemistry of Explosives and Propellants at High Temperature: HMX, RDX and BAMO," *Philosophical Transactions of the Royal Society of London, Series A: Mathematical and Physical Sciences*, Vol. 339, No. 1631, 1992, pp. 377–385.

[6]Miyazaki, T., and Kubota, N., "Energetics of BAMO," *Propellants, Explosives, Pyrotechnics*, Vol. 17, 1992, pp. 5–9.

[7]Busch, K. L., Glish, G. L., and McLuckey, S. A., *Mass Spectrometry/Mass Spectrometry*, VCH Publishers, Inc., New York, 1988.

[8]*Eight Peak Index of Mass Spectra*, Vols. 1–3, The Mass Spectrometry Data Centre, The Royal Society of Chemistry, The University, Nottingham, England, UK, 1993.

[9]Lee, Y. J., "A Study of the Physical and Chemical Processes Governing CO_2 Laser-Induced Pyrolysis and Combustion of RDX, BAMO, RDX/BAMO Pseudo-Propellants," Ph.D. Dissertation, Dept. of Mechanical Engineering, Pennsylvania State Univ., University Park, PA, 1996.

[10]Litzinger, T. A., Fetherolf, B. L., Lee, Y. J., and Tang, C.-J., "Study of Gas-Phase Chemistry of RDX: Experiments and Modeling," *Journal of Propulsion and Power*, Vol. 11, No. 4, 1995, pp. 698–703.

[11]Tang, C.-J., Lee, Y. J., and Litzinger, T. A., "A Study of Gas-Phase Processes During the Deflagration of RDX Composite Propellants Using a Triple Quadrupole Mass-Spectrometer," 31st JANNAF Combustion Meeting, Oct. 1994.

[12]Bobeldijk, M., Van der Zande, W. J., and Kistemaker, P. G., "Simple Models for the Calculation of Photoionization and Electron Impact Ionization Cross Sections of Polyatomic Molecules," *Chemical Physics*, Vol. 179, No. 2, 1994, pp. 125–130.

[13]Lee, Y. J., Tang, C.-J., Kudva, G., and Litzinger, T. A., "Thermal Decomposition of BAMO and RDX/BAMO Pseudo-Propellants," 33rd JANNAF Combustion Meeting, Nov. 1996.

[14]*Catalog Handbook of Fine Chemicals*, Aldrich Chemical Company, Inc., Milwaukee, WI, 1994–1995.

[15]Arisawa, H., and Brill, T., "Thermal Decomposition of Energetic Materials 71. Structure-Decomposition and Kinetic Relationships in Flash Pyrolysis of Glycidyl Azide Polymer (GAP), *Combustion and Flame* (to be published).